Available online at www.sciencedirect.com
SCIENCE DIRECT®
Physica E 18 (2003) 56–59
PHYSICA E
www.elsevier.com/locate/physe

Tunable Fano system: a quantum dot embedded in an Aharonov–Bohm ring

Kensuke Kobayashi*, Hisashi Aikawa, Shingo Katsumoto, Yasuhiro Iye

Institute for Solid State Physics, University of Tokyo, 5-1-5 Kashiwanoha, Chiba 277-8581, Japan

Abstract

The Fano effect illustrates how the quantum interference occurs between a localized state and the energy continuum. While this phenomenon is ubiquitously observed in many different physical systems, it has been difficult to obtain a Fano system with desired parameters. We have realized for the first time a tunable Fano system by fabricating a quantum dot (QD) embedded in an Aharonov–Bohm interferometer on a two-dimensional electron gas. In the Coulomb oscillation, clear asymmetric lineshapes were observed, which manifest the formation of the Fano state, i.e., a mixture of the localized-continuum states. The Fano interference can be tuned through the phase of the electrons by the magnetic flux piercing the ring, revealing that Fano's asymmetric parameter q should be complex.

Keywords: Fano effect; Quantum dot; Aharonov–Bohm ring; Coherence

1. Introduction

In 1961, Fano proposed that a system where exist a discrete state and the continuum energy state possesses a characteristic transition probability around the discrete energy level [1]. The essence lies in the quantum interference between the two configurations in the transition process into the final states with the same energy as sketched in Fig. 1(a): one directly through the continuum and the other through the resonance level arising around the discrete state. This "configuration interaction" yields the peculiar asymmetric line shape in the transition probability T from an arbitrary initial state given by

$$T(\tilde{\varepsilon}) \propto \frac{(\tilde{\varepsilon}+q)^2}{\tilde{\varepsilon}^2+1}, \quad \tilde{\varepsilon} = \frac{\varepsilon-\varepsilon_0}{\Gamma/2}, \tag{1}$$

where ε_0 is the energy level of the resonance state and Γ is its width. The parameter q, which is the ratio of the matrix elements linking the initial state to the discrete and continuum parts of the final state, serves as a measure of the degree of coupling between both. q is usually treated as real.

The Fano effect is a ubiquitous phenomenon observed in wide-ranging spectroscopy as reported in, to mention only a few examples, Refs. [2–5]. It can be viewed as a theory describing how a localized state embedded in the continuum acquires itinerancy over the system [6]. An experiment on a single site, therefore, would reveal this fundamental process in a more transparent way. While the single-site Fano effect has been reported in the scanning tunneling spectroscopy study of an atom on the surface [7,8] or in transport through a quantum dot (QD) [9], it has been difficult to obtain a Fano system with variable parameters.

In the present work, we report the first tunable Fano experiment realized in a QD embedded in an Aharonov–Bohm (AB) interferometer. We have clarified characteristic transport properties arising from this effect, such as the delocalization of the discrete level and the excitation spectra of the Fano system. Magnetic field control of the relative phase between a localized state and the continuum indicates that Fano's parameter q should be extended to be complex rather than real.

2. Experiments

We designed an AB ring with a QD in one of its arms as seen in Fig. 1(b). The AB ring is essentially a double-slit

* Corresponding author.
E-mail address: knsk@issp.u-tokyo.ac.jp (K. Kobayashi).

1386-9477/03/$ - see front matter
doi:10.1016/S1386-9477(02)00960-8

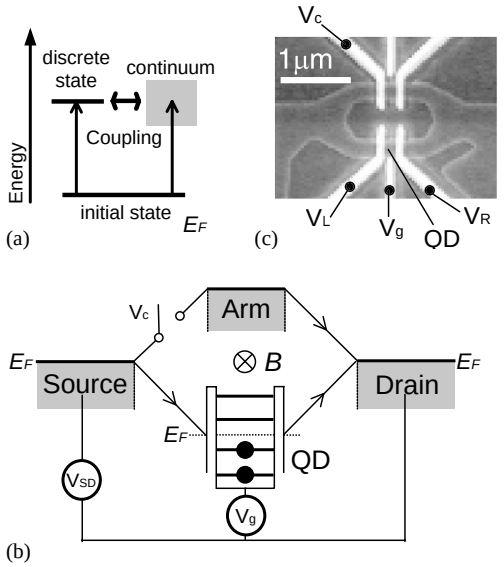

Fig. 1. (a) The principle of the Fano effect. (b) Schematic representation of the experimental setup. (c) Scanning electron micrograph of the correspondent device fabricated by wet-etching the 2DEG at an AlGaAs/GaAs heterostructure. The three gates (V_R, V_L, and V_g) at the lower arm are used for controlling the QD and the gate at the upper arm is for V_C.

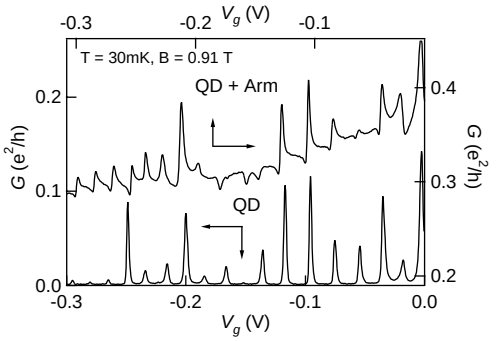

Fig. 2. Typical Coulomb oscillation at $V_C = -0.12$ V with the arm pinched off, and asymmetric Coulomb oscillation at $V_C = -0.086$ V with the arm transmissible. The latter shows a clear Fano effect. Both of them were obtained at $T = 30$ mK and $B = 0.91$ T.

interferometer of electrons. In contrast, the QD is an "artificial atom" [10] connected to the leads with tunneling barriers, whose single-particle level can be controlled electro-statically by the gate voltage (V_g). Thus, an electron injected from the source traverses our "modified" AB interferometer along two different paths through the continuum in the arm and the discrete level inside the QD and interferes before the drain. If the coherence of the electron is fully maintained during the traverse over the system, this interferometer is exactly a realization of the Fano system [11–14]. Unlike the other Fano systems it is unique in that it is controllable through several parameters; V_g (the position of the discrete level inside the QD), the control gate voltage V_C (the coupling between the continuum and the discrete levels), and the magnetic field B penetrating the ring (the phase difference between two paths).

Fig. 1(c) shows the fabricated Fano system on a two-dimensional electron gas (2DEG) system at an AlGaAs/GaAs heterostructure (mobility $= 9 \times 10^5$ cm^2/V s and sheet carrier density $= 3.8 \times 10^{11}$/cm^2). This sample geometry is similar to those in previous studies [15–18]. The ring-shaped conductive region was formed by wet-etching the 2DEG. The white regions indicate the Au/Ti metallic gates deposited to control the device. The QD can be defined in the lower arm by tuning the side-gate voltages (V_L and V_R) and its single-particle level can be tuned by V_G. The gate in the upper arm is V_C for switching the transition through the continuum state on and off. Measurements were performed in a dilution refrigerator by a standard lock-in technique in the two-terminal setup with an excitation voltage of 10 μV (80 Hz) between the source and the drain.

3. Results and discussions

The lower panel of Fig. 2 shows the conductance G observed with the upper arm pinched off. The pronounced peaks are due to a typical Coulomb oscillation of a simple QD. The small irregularity of the peak positions reflects that of the addition energy and supports the occurrence of transport through each single level inside the QD. When we made the upper arm conductive, a clear one-to-one correspondence is observed between the two results in Fig. 2 since the control gate and the QD are well separated electrostatically. This ensures that the discreteness of the energy levels in the QD is maintained. The line shapes of the oscillation in the upper panel of Fig. 2, however, are very asymmetric with the intensity minima very close to the intensity maxima. Moreover, even a simple dip structure rather than a peak appears at several positions.

The asymmetric line shape observed above is a clear sign of the Fano effect. Indeed, each peak was found to be well fitted by the Fano line shape Eq. (1). The dip structure, which corresponds to $|q| < 1$, indicates a strong destructive interference, supporting that the electron passing the QD retains sufficient coherency to interfere with the one passing the arm in spite of the significant charging effect inside and around the QD. This is in contrast with the previous reports [15–18], where the coherence was limited to a fraction of the transmission through the QD. The Fano effect was found to be prominent within several specific magnetic field ranges around $B \sim 0.3$, 0.9, and 1.2 T and to be less pronounced in the other ranges, while the reason is not fully understood at this moment.

The essences of the Fano effect lies in the existence of the interference. To see this, we can introduce decoherence into

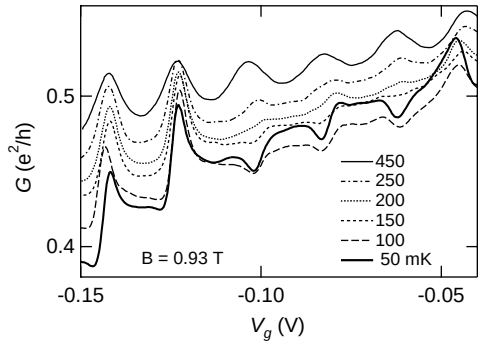

Fig. 3. The Fano effect measured at several temperatures at $B = 0.93$ T. It gradually disappears as the temperature increases.

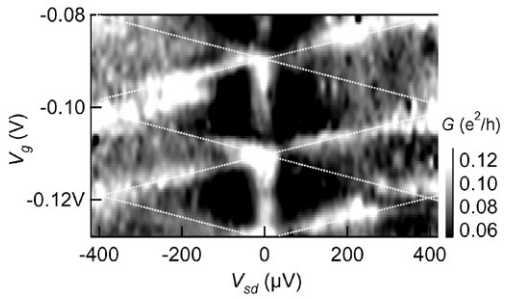

Fig. 4. Differential conductance obtained as a function of V_g at $T = 30$ mK and $B = 0.92$ T. The zero-bias conductance peak exists in the CB region with a Coulomb diamond superimposed. The edge of the CB region is emphasized with white dashed lines. Incoherent contribution from the differential conductance of the upper arm, which shows slight non-Ohmic behavior at finite V_{sd}, has been subtracted from the data.

the system, e.g., by increasing the temperature. Then, asymmetric Fano line shapes gradually evolved into a Lorentzian line shape corresponding to $|q| \to \infty$ as seen in Fig. 3. Hence, at $T \geqslant 450$ mK, the system is simply a classical parallel circuit of the QD and the arm.

The differential conductance at the lowest temperature as a function of both source–drain bias (V_{sd}) and V_g also shows a behavior peculiar to this effect. Fig. 4 depicts that the resonating conductance peak of the width ~ 70 μeV (white colored region) stretches along the line of $V_{sd} = 0$ V with the Coulomb diamond superimposed. The zero-bias structure is consistent with the previous report for the Fano effect in a simple QD [9]. The appearance of the zero-bias conductance peak even in the Coulomb blockade (CB) region indicates that the transmission through the QD is now allowed due to the aid of the continuum in the opposite arm.

The largest advantage of the present system over the other Fano systems is the spatial separation between the discrete level and the continuum, which allows us to control Fano interference via the magnetic field piercing the ring. As shown

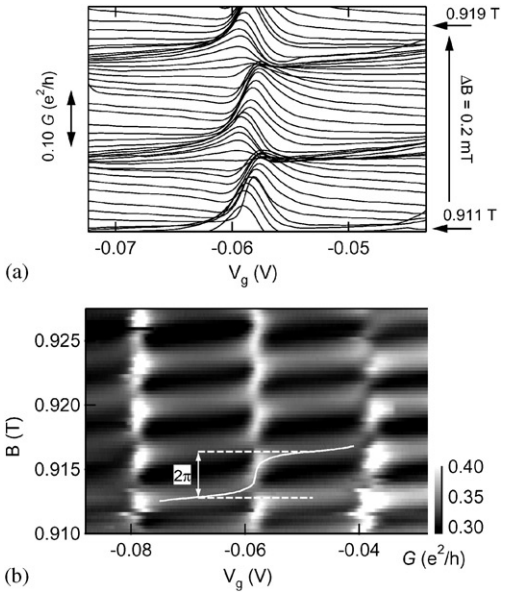

Fig. 5. (a) Conductance of the Fano peaks at several magnetic fields around 0.91 T at 30 mK. The curves are incrementally shifted upwards. (b) Conductance of the Fano peaks as a function of V_g and B at 30 mK. AB oscillation exists even at the midpoint of the resonances. The white line represents the AB phase as a function of V_g. Note that the AB phase changes by 2π through the resonance, and all the resonances are in phase.

in Figs. 5(a) and (b), the line shape changes periodically with the AB period of ~ 3.8 mT, which agrees with that expected from the ring dimension. Fig. 5(a) shows that, as B varies, an asymmetric line shape with negative q continuously changes to a symmetric one and then to an asymmetric one with positive q; the sign of interference can be controlled by the AB effect. Since the magnetic field mainly affects the phase difference between the two paths through the resonant state and the continuum, the aforementioned periodic behavior is most likely explained systematically by introducing a complex number q whose argument is a function of B or the AB flux, although an expression of such q applicable to our case is not known at present. Here, Eq. (1) is generalized as follows:

$$T(\tilde{\varepsilon}) \propto \frac{|\tilde{\varepsilon} + q|^2}{\tilde{\varepsilon}^2 + 1} = \frac{(\tilde{\varepsilon} + \mathrm{Re}\, q)^2 + (\mathrm{Im}\, q)^2}{\tilde{\varepsilon}^2 + 1}. \quad (2)$$

Qualitatively, even when the coupling strength $|q|$ is almost independent of B, the B-dependence of $\arg(q)$ yields asymmetric and symmetric line shapes of G for $\mathrm{Re}\, q \gg \mathrm{Im}\, q$ and $\mathrm{Re}\, q \ll \mathrm{Im}\, q$, respectively. While the expression of Eq. (2) does not at all conflict with the Fano theory [1], the asymmetric parameter q has been implicitly treated as a real number in his original work and most of the subsequent studies. We would like to emphasize that such a treatment is valid only when the system has the time-reversal symmetry and

thus the matrix elements defining q can be taken as real. Our experiment indicates that when this condition is broken, for example, under the magnetic field, q should be a complex number, which has not been explicitly recognized.

Fig. 5(b) represents the result over three Fano resonances in the V_g–B plane. Clear AB oscillation is observed even at the conductance valley between the resonant peaks. This provides another evidence that the state in the QD becomes delocalized with the aid of the continuum. In Fig. 5(b) we also plot the conductance maximum as a function of V_g, where the phase changes by 2π rapidly but continuously across the resonance. Since the measurement was performed in the two-terminal setup that allows only phase changes by multiples of π due to reasons of symmetry, the continuous behavior of the AB phase is unexpected, but may be attributed to the breaking of the time-reversal symmetry [19]. The AB phase changes only slightly at the conductance valley and, therefore, all the adjacent Fano resonances are in phase, indicating that the resonance peaks are correlated to each other [19]. Several theoretical predictions on the behavior of the AB phase in the Fano system have been reported [11–14], there are still features left to be explained theoretically.

4. Conclusion

We report the first convincing demonstration of a tunable Fano effect realized in the QD-AB-ring hybrid system. Peculiar transport properties such as the asymmetric line shapes of the Coulomb peak and the zero-bias resonance in the differential conductance are attributed to this effect due to the coherence between the discrete level in the QD and the continuum in the arm of the ring. The zero-bias peak in the differential conductance and the significant AB amplitude at the Coulomb valley present clear evidence that the localized state in the QD acquires itinerancy even in the CB region with the aid of the continuum. Controlling of the Fano line shape by the magnetic field has revealed that the Fano parameter q will be extended to a complex number, which might shed a new light on the analysis in general spectroscopy.

Acknowledgements

This work is supported by a Grant-in-Aid for Scientific Research and by a Grant-in-Aid for COE Research ("Quantum Dot and Its Application") from the Ministry of Education, Culture, Sports, Science, and Technology of Japan.

References

[1] U. Fano, Phys. Rev. 124 (1961) 1866.
[2] R.K. Adair, C.K. Bockelman, R.E. Peterson, Phys. Rev. 76 (1949) 308.
[3] U. Fano, A.R.P. Rau, Atomic Collisions and Spectra, Academic Press, Orland, 1986.
[4] F. Cerdeira, T.A. Fjeldly, M. Cardona, Phys. Rev. B 8 (1973) 4734.
[5] J. Faist, F. Capasso, C. Sirtori, K.W. West, L.N. Pfeiffer, Nature 390 (1997) 589.
[6] G.D. Mahan, Many-Particle Physics, Plenum Press, New York, 1990.
[7] V. Madhavan, W. Chen, T. Jamneala, M.F. Crommie, N.S. Wingreen, Science 280 (1998) 567.
[8] J. Li, W.D. Schneider, R. Berndt, B. Delley, Phys. Rev. Lett. 80 (1998) 2893.
[9] J. Göres, D. Goldhaber-Gordon, S. Heemeyer, M.A. Kastner Hadas Shtrikman, D. Mahalu, U. Meirav, Phys. Rev. B 62 (2000) 2188.
[10] M. Kastner, Phys. Today 46 (1993) 24.
[11] C.-M. Ryu, S.Y. Cho, Phys. Rev. B 58 (1998) 3572.
[12] K. Kang, Phys. Rev. B 59 (1999) 4608.
[13] O. Entin-Wohlman, A. Aharony, A.Y. Imry, Y. Levinson, cond-mat/0109328 (2001).
[14] T.-S. Kim, S.-Y. Cho, C.-K. Kim, C.-M. Ryu, cond-mat/0110395 (2001).
[15] A. Yacoby, M. Heiblum, D. Mahalu, H. Shtrikman, Phys. Rev. Lett. 74 (1995) 4047.
[16] R. Schuster, E. Buks, M. Heiblum, D. Mahalu, V. Umansky, H. Shtrikman, Nature 385 (1997) 417.
[17] W.G. van der Wiel, S. De Franceschi, T. Fujisawa, J.M. Elzerman, S. Tarucha, L.P. Kouwenhoven, Science 289 (2000) 2105.
[18] Yang Ji, M. Heiblum, D. Sprinzak, D. Mahalu, Hadas Shtrikman, Science 290 (2000) 779.
[19] H.-W. Lee, Phys. Rev. Lett. 82 (1999) 2358.